Influence of Boundary Conditions on the Modal Characteristics of Thin Cylindrical Shells

KEVIN FORSBERG*
Lockheed Missiles and Space Company, Palo Alto, Calif.

The modal characteristics of thin cylindrical shells have previously been determined only for three sets of boundary conditions. In the present analysis, all sixteen sets of homogeneous boundary conditions have been examined at each end of the shell (each set contains four conditions). The equations of motion developed by Flügge for thin, circular cylindrical shells are used. The general solution to these equations can easily be written down. One can select a circumferential nodal pattern, eight boundary conditions, and a length of shell, and then iterate numerically to find the frequency of vibration that will meet these conditions. The advantage of this approach is that one can obtain a solution to the basic equations for any boundary conditions desired. Results indicate that, contrary to the rather common assumption, the condition placed on the longitudinal displacement u in many cases is more influential than restrictions on the slope $\partial w/\partial x$ or moment M_x. It has been found that even for long cylinders (length to radius ratio of 40 or more) the minimum natural frequency may differ by more than 50% depending upon whether $u = 0$ or the longitudinal stress resultant $N_x = 0$ at both ends.

Nomenclature

a	=	radius of cylinder
h	=	thickness of cylinder wall
k	=	$h^2/12a^2$
l	=	length of shell
m	=	number of axial half-waves
n	=	number of circumferential waves
u	=	longitudinal displacement
v	=	tangential displacement
w	=	radial displacement
x	=	dimensionless axial coordinate, ξ/a
E	=	Young's modulus of elasticity
$M_x, M_{x\varphi}, N_x, N_{x\varphi}, Q_x$	=	stress resultants, see Fig. 1
S_x	=	$Q_x + \partial M_{x\varphi}/a\partial\varphi$
T_x	=	$N_x - M_{x\varphi}/a$
γ^2	=	$\rho a^2(1 - \nu^2)/E$
ν	=	Poisson's ratio
ξ	=	axial coordinate
ρ	=	mass density of shell material
φ	=	circumferential coordinate
ω	=	circular frequency
ω_0	=	lowest extensional frequency of a ring in plane strain, $= 1/\gamma$
$(\ )'$	=	$\partial(\ldots)/\partial x$
$(\ )\cdot$	=	$\partial(\ldots)/\partial\varphi$

Introduction

THE determination of the modal characteristics for vibrations of thin cylindrical shells is a problem of great technical interest. However, in spite of the great number of papers devoted to this topic,[1] only three sets of boundary conditions (i.e., one set for a force-free end and two other sets loosely called "freely supported" end and "clamped" end) have been considered in the literature. Additionally there appears to be no discussion of how the modal characteristics are altered when longitudinal displacement is prevented at the ends.

The primary contribution of this paper is the presentation of results obtained from an exact solution of the basic differential equations of motion. The method, which was outlined by Flügge in 1934, requires numerical evaluation of an eighth-order determinant to find its eigenvalues, and this is certainly the reason this approach was not feasible before the advent of a high-speed digital computer. Although the method requires numerical computation, the results are exact in the same sense that the numerical solution to the transcendental frequency equation for a beam yields an exact solution.

This study is identical in approach with the recently published work of Sobel[2] on the closely related area of stability of cylindrical shells. The results of these two independent studies lead to the same conclusions regarding the importance of the various boundary conditions.

The major purpose of the present report is to determine the ranges of the length-to-radius ratio l/a and radius-to-thickness ratio a/h for which a change in the boundary conditions will appreciably alter the modal characteristics. The modal behavior of a simply supported shell without axial constraint is used as the reference for comparison. This investigation will be directed into three areas: 1) the effect of the various boundary conditions on the frequency envelope (10 cases are considered here); 2) a study of a portion of the over-all frequency pattern for one value of a/h and for two sets of boundary conditions; and 3) a brief study of the modal stress resultants for several cases.

This study will be presented in two parts. The second part, which is in preparation, will consider the cases for which $n = 0$ and $n = 1$. Also in the second part a brief investigation will be made of shells having one or both ends entirely force free (all values of n will be considered). A comparison with experimental data will be made for a cylinder having force-free ends.

The Flügge equations used in the present analysis are based on the usual assumptions of linear thin shell theory, i.e., that the shell is thin (usually considered to mean $a/h > 10$), of constant wall thickness, and of a linear, homogeneous, isotropic material. The results apply only for small deflections and, since the effects of shear distortion and rotatory inertia of the shell wall have been neglected, the results apply only when the half-wave length of the mode shape is

Presented as Preprint 64-77 at the AIAA Aerospace Sciences Meeting, New York, January 20–22, 1964; revision received July 27, 1964. This work was partially sponsored by the Lockheed Independent Research Program. The author would like to express his appreciation to C. W. Coale for the helpful advice given during the writing of this paper.

* Research Specialist, Aerospace Sciences Laboratory. Member AIAA.

more than ten times the shell wall thickness ($l/ma > 10\ h/a$, $\pi/n > 10\ h/a$), where m and $2n$ are the number of axial and circumferential half-waves.

Method of Solution

The present analysis is based on the following equations of motion developed by Flügge[3] for free vibrations of thin, circular cylindrical shells (see Fig. 1):

$$\left.\begin{aligned}
&u'' + \frac{1-\nu}{2}(1+k)u^{\cdot\cdot} + \frac{1+\nu}{2}v'^{\cdot} - kw''' + \\
&\qquad \frac{1-\nu}{2}kw'^{\cdot\cdot} + \nu w' - \gamma^2\frac{\partial^2 u}{\partial t^2} = 0 \\
&\frac{1+\nu}{2}u'^{\cdot} + v^{\cdot\cdot} + \frac{1-\nu}{2}(1+3k)v'' - \\
&\qquad \frac{3-\nu}{2}kw''^{\cdot} + w^{\cdot} - \gamma^2\frac{\partial^2 v}{\partial t^2} = 0 \\
&-ku''' + \frac{1-\nu}{2}ku'^{\cdot\cdot} + \nu u' - \frac{3-\nu}{2}kv''^{\cdot} + v^{\cdot} + \\
&w + k[w^{IV} + 2w''^{\cdot\cdot} + w^{\cdot\cdot\cdot\cdot} + 2w^{\cdot\cdot} + w] + \gamma^2\frac{\partial^2 w}{\partial t^2} = 0
\end{aligned}\right\} \quad (1)$$

where

$$(\ )' = \partial(\ )/\partial x \qquad (\ )^{\cdot} = \partial(\ )/\partial\varphi$$
$$\gamma^2 = \rho a^2(1-\nu^2)/E \qquad k = h^2/12a^2$$

For a complete cylinder, the general solution for modal vibration can easily be written in the following form:

$$\begin{aligned}
u &= \left(\sum_{n=0}^{\infty}\sum_{s=1}^{8}\alpha_{sn}A_{sn}e^{\lambda_{sn}x}\cos n\varphi\right)e^{i\omega t} \\
v &= \left(\sum_{n=0}^{\infty}\sum_{s=1}^{8}\beta_{sn}A_{sn}e^{\lambda_{sn}x}\sin n\varphi\right)e^{i\omega t} \\
w &= \left(\sum_{n=0}^{\infty}\sum_{s=1}^{8}A_{sn}e^{\lambda_{sn}}\ \cos n\varphi\right)e^{i\omega t}
\end{aligned} \quad (2)$$

The arbitrary constants A_{sn} will be evaluated by considering the boundary conditions at each end of the shell. Any of the boundary conditions can be a general function of the circumferential coordinate φ and can be expressed by a Fourier series in φ. Thus, in the general case of nonuniform boundary conditions, the frequency of modal vibration ω will depend upon all of the harmonics n. For the special cases in which the boundary conditions depend on only one harmonic, or when the boundary conditions are homogeneous, the modal frequency will be a function of a single value of n, and the summation over n in Eq. (2) can be discarded. Only this latter case will be considered in the present paper. Thus the index n will be dropped.

Substitution of these expressions into the homogeneous differential equations leads to an eighth-order algebraic equation for λ_s:

$$\lambda_s^8 + g_{s6}\lambda_s^6 + g_{s4}\lambda_s^4 + g_{s2}\lambda_s^2 + g_{s0} = 0 \quad (3)$$

where

$$g_{sk} = g_{sk}\ (h/a,\ \nu,\ n,\ \omega)$$

The preceding solution is readily obtainable from Ref. 3. In contrast to the associated statics problem for which the roots of Eq. (3) are, in general, all complex, it can be shown that the solution for the vibration problem will usually have the form

$$\lambda = \pm a,\ \pm ib,\ \pm(c \pm id)$$

where a, b, c, d are real quantities. For a finite shell, there will always be at least two roots of the form $(\pm ib)$. This leads to a solution of the form

$$\begin{aligned}
w = \{&C_1e^{ax} + C_2e^{-ax} + C_3\cos bx + C_4\sin bx + \\
&e^{cx}(C_5\cos dx + C_6\sin dx) + e^{-cx}(C_7\cos dx + \\
&C_8\sin dx)\}\cos n\varphi e^{i\omega t}
\end{aligned} \quad (4)$$

with similar expressions for u and v. Note that Eq. (4) has been rewritten so that the complex constants A_s have been replaced by real constants C_s. The expressions for u and v involve combinations of the constants C_s and the real and imaginary parts of α_s or β_s. It should be noted that the parameters α_s and β_s depend on λ_s, h/a, ν, n, and ω. When the solutions to Eq. (3) are obtained, α_s and β_s can be evaluated.

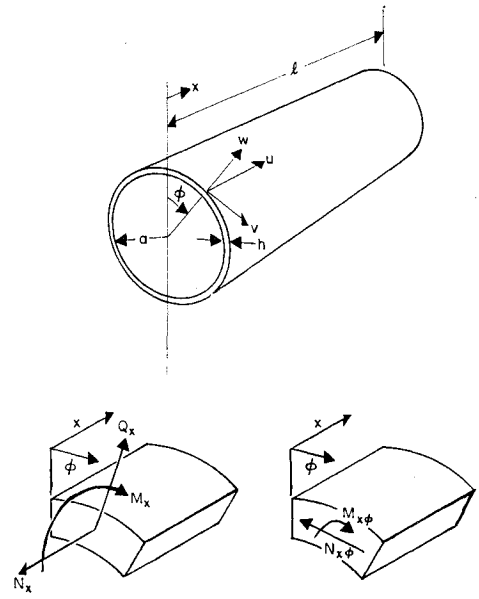

Fig. 1 Coordinate system and shell element.

Once the boundary conditions are specified (four at each end of the shell), the problem is entirely determined. The detailed statement of these conditions leads directly to eight equations for the eight unknown constants C_s. These equations involve the four quantities a, b, c, and d. Since the boundary conditions are homogeneous, the determinant D of these equations must be zero for a nontrivial solution.

It does not appear feasible to seek analytic expressions for the quantities a, b, c, and d. Thus, at this point in the analysis, a numerical evaluation of the solution is introduced. We now select a given shell (i.e., fix a/h, l/a, ν), an assumed number of circumferential waves n, and a specific set of boundary conditions at each end. Starting from some initial estimate for the frequency ω, we can iterate to find the values of ω which will make the determinant D go to zero. We can cover the entire range of problems of interest by varying the initial input to the determinant, i.e., by varying a/h, l/a, ν, n, or the boundary conditions.

No assumptions or simplifications beyond those underlying Eqs. (1) have been introduced in the numerical evaluation, and the solution can be obtained with any desired degree of accuracy. In the present instance, the frequency was determined to six significant figures. Such accuracy, required only for intermediate computations, is necessary in order to obtain accurate values for the mode shapes and corresponding modal stress resultants. The final result is only meaningful for three or four significant figures of course. The number of iterations required for convergence is greatly reduced if good initial estimates are available. The solutions developed by Arnold and Warburton[4, 5] are excellent for this purpose. It should be noted that, for any given modal pattern (fixed number of axial half-waves m and cir-

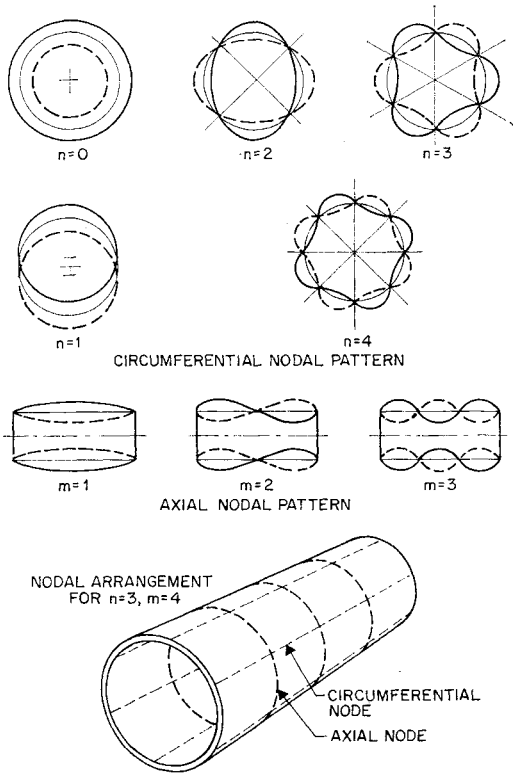

Fig. 2 Nodal patterns.

cumferential waves n), there are three frequencies, corresponding to different amplitude ratios in u, v, and w.[4] If longitudinal and tangential inertia terms are omitted, there will be only one value of ω for each pair of m and n. For $n \geq 1$, this eigenvalue is an approximation to the lowest of the three frequencies just mentioned. In the present approach, the number of axial half-waves m cannot be specified conveniently in advance, and thus one must take care to determine the mode shape as well as the frequency in each instance, since there are an infinite number of eigenvalues for any fixed set of values of n, a/h, l/a, and ν. Although it is possible for two mode shapes to have identical natural frequencies, this can occur only if they have different values of n. For a given number of circumferential waves, the frequency increases monotonically as the number of axial waves increases. However, for long shells the frequencies for $m = 1, 2, 3, \ldots$, are very closely spaced; the longer the shell the closer are the frequencies of adjacent axial modes.

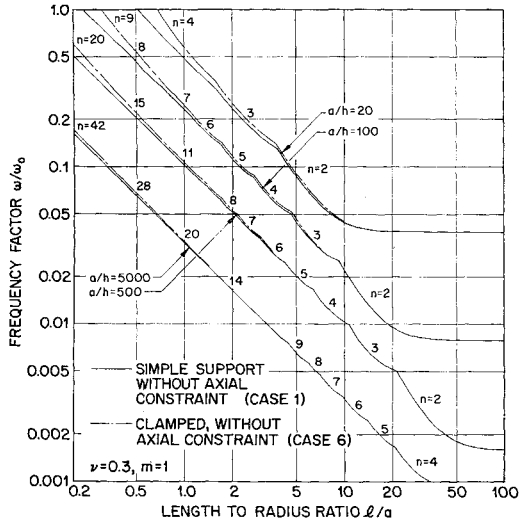

Fig. 3 Frequency envelope, cases 1 and 6.

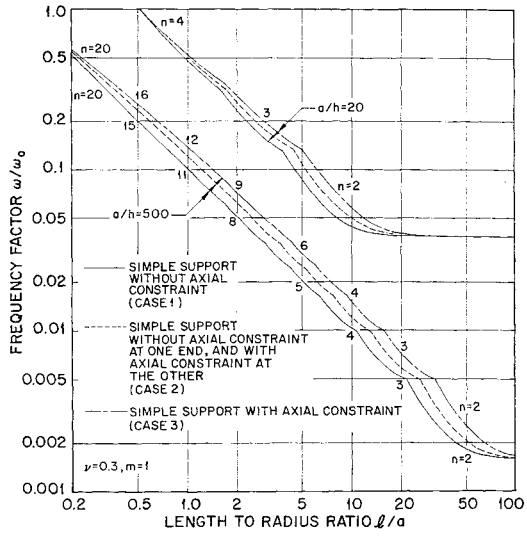

Fig. 4 Frequency envelope, cases 1–3.

Finally it should be pointed out that, for mode shapes in which $n \geq 2$, if one starts from a zero frequency, the minimum nonzero eigenvalue obtained will be that of an infinite cylinder (or a ring in a state of plane strain). This value is independent of the axial wavelength (and hence independent of the boundary conditions) and represents the asymptotic value for a given n, a/h, and ν as $l/a \rightarrow \infty$. It does not, in general, represent a solution for a finite shell. The numerical computation was done on an IBM 7094 computer.

Boundary Conditions

There are 16 possible sets of homogeneous boundary conditions which can be specified independently at each end of the shell. These consist of all combinations of the following:

$$w = 0 \text{ or } S_x = Q_x + (1/a)\,\partial M_{x\varphi}/\partial\varphi = 0 \tag{5a}$$

$$\partial w/\partial x = 0 \text{ or } M_x = 0 \tag{5b}$$

$$u = 0 \text{ or } N_x = 0 \tag{5c}$$

$$v = 0 \text{ or } T_x = N_{x\varphi} - (1/a)\,M_{x\varphi} = 0 \tag{5d}$$

(For a discussion of the origin of the force boundary conditions indicated in Eqs. (5a) and (5d), see Ref. 3, p. 233.) For completeness, all 16 sets of conditions were studied in the course of the present investigation for shells having the same boundary conditions at both ends. Free ends (cases with $S_x = 0$) will be discussed in a subsequent paper. Additionally, selected combinations of one set at one end and a different set at the other were examined.

The significant findings of this study can be summarized by discussing the ten cases indicated in Table 1. Certain symbols used therein are defined in Fig. 1. The exact solution for case 1 has been discussed in detail by Arnold and Warburton.[4] It is included here for comparison. Arnold and Warburton also presented an approximate solution[5] for case 7. A comparison of their results with the present analysis is given below.

Discussion of Results

Frequency Envelope for $n \geq 2$

The general character of the various mode shapes is indicated in Fig. 2. Modes for which $n < 2$ have a somewhat different behavior from those having $n \geq 2$ and will be treated at a later date.

For any fixed values of n and m, there are three natural frequencies corresponding to three mode shapes (having different u, v, w amplitude ratios). The asymptotic values of these frequencies for long axial wavelengths are:

Flexural Vibrations of a Ring ($w_{max} = nv_{max}$, $u = 0$)

$$(\omega_1/\omega_0)^2 = (h^2/12a^2)n^2(n^2 - 1)^2/(n^2 + 1)$$

Axial Shear Vibration ($w = v = 0$)

$$(\omega_2/\omega_0)^2 = (1 - \nu)n^2/2$$

Extensional Vibrations of Ring ($v_{max} = nw_{max}$, $u = 0$)

$$(\omega_3/\omega_0)^2 = n^2 + 1$$

In general, two of these three frequencies are several orders of magnitude higher than the minimum value and hence are not usually of immediate interest.

These higher frequencies will arise only if all three inertia terms are retained in Eqs. (1). Although these higher frequencies are not to be studied here, all three inertia terms have been retained in developing the results presented herein. One approach for determining the region of influence of the various boundary conditions on the modal behavior of cylindrical shells consists of looking at the minimum natural frequency (which is the envelope of the frequency curves drawn for constant values of n). The value of n varies from point to point as indicated on the curves shown in Figs. 3–7. Moreover, for a given shell of fixed length, changing the boundary conditions may alter the value of n associated with the minimum frequency. Since the minimum frequency always occurs for a mode having one axial half-wave ($m = 1$), Figs. 3–7 are all drawn for $m = 1$.

One should keep in mind the fact that, for long shells, the minimum frequency will occur for $n = 1$. The values of l/a for which this change takes place depend upon a/h. For $a/h = 20$, the crossover occurs for $l/a = 12$ to 18; for $a/h = 5000$, the change occurs for $l/a > 100$.

The effect of clamping ($\partial w/\partial x = 0$) is illustrated in Fig. 3, in which the minimum frequency for a simply supported shell without axial constraint is compared with that of a clamped shell without axial constraint. Clearly, the effect of clamping rapidly diminishes as the length increases. The magnitude of the increase in minimum frequency due to clamping is quite small for all but very short shells ($l/a < 1$).

The influence of axial constraint ($u = 0$) is illustrated in Fig. 4. Here the minimum frequency for a simply supported shell without axial constraint is compared with that of a simply supported shell with axial constraint at one or both ends. In direct contrast to the previous case, the effect of axial constraint is significant even for very long shells and for all values of a/h. Note that the minimum frequency for case 3 is about 40 to 60% higher than in that of case 1 through-

Table 1 List of boundary conditions used in present analysis

Case no.	Description	Boundary conditions $x = 0$	Boundary conditions $x = l/a$
1	Simple support without axial constraint (called "freely supported" in Ref. 3)	$w = 0$ $v = 0$ $M_x = 0$ $N_x = 0$	$w = 0$ $v = 0$ $M_x = 0$ $N_x = 0$
2	Simple support without axial constraint at one end, with axial constraint at other	$w = 0$ $v = 0$ $M_x = 0$ $N_x = 0$	$w = 0$ $v = 0$ $M_x = 0$ $u = 0$
3	Simple support with axial constraint	$w = 0$ $u = 0$ $v = 0$ $M_x = 0$	$w = 0$ $u = 0$ $v = 0$ $M_x = 0$
4	Simple support, no tangential constraint (similar to case 1, with $v \neq 0$)	$w = 0$ $M_x = 0$ $N_x = 0$ $T_x = 0$	$w = 0$ $M_x = 0$ $N_x = 0$ $T_x = 0$
5	Simple support, axial constraint but no tangential constraint (similar to case 3, with $v \neq 0$)	$w = 0$ $u = 0$ $M_x = 0$ $T_x = 0$	$w = 0$ $u = 0$ $M_x = 0$ $T_x = 0$
6	Clamped end, without axial constraint	$w = 0$ $w' = 0$ $v = 0$ $N_x = 0$	$w = 0$ $w' = 0$ $v = 0$ $N_x = 0$
7	Clamped end, with axial constraint (called "fixed end" in Ref. 4)	$w = 0$ $w' = 0$ $u = 0$ $v = 0$	$w = 0$ $w' = 0$ $u = 0$ $v = 0$
8	Clamped end, no tangential constraint (similar to case 6, but with $v \neq 0$)	$w = 0$ $w' = 0$ $N_x = 0$ $T_x = 0$	$w = 0$ $w' = 0$ $N_x = 0$ $T_x = 0$
9	Clamped end, with axial constraint but no tangential constraint (similar to case 7, but with $v \neq 0$)	$w = 0$ $w' = 0$ $u = 0$ $T_x = 0$	$w = 0$ $w' = 0$ $u = 0$ $T_x = 0$
10	Simple support without axial constraint at one end, clamped with axial constraint at the other end	$w = 0$ $v = 0$ $M_x = 0$ $N_x = 0$	$w = 0$ $v = 0$ $w' = 0$ $u = 0$

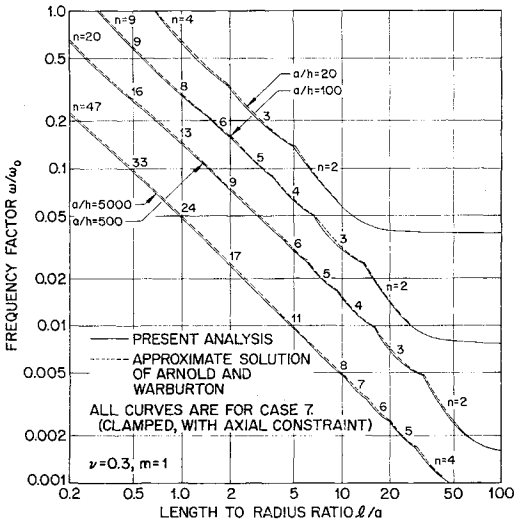

Fig. 5 Frequency envelope, case 7 and Arnold and Warburton's approximate solution.

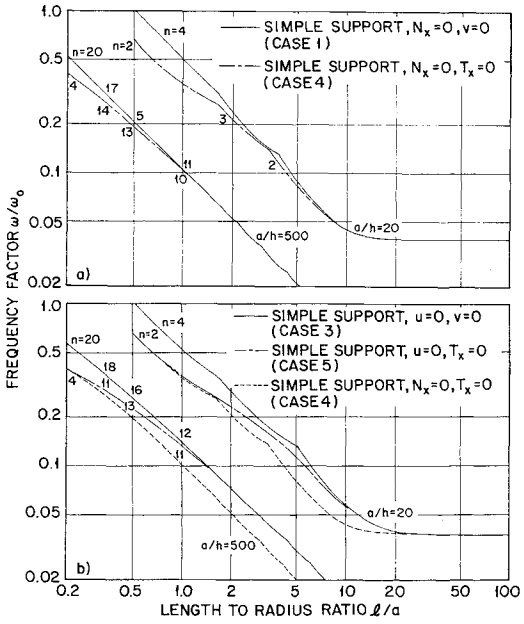

Fig. 6 Frequency envelope, cases 1 and 3–5.

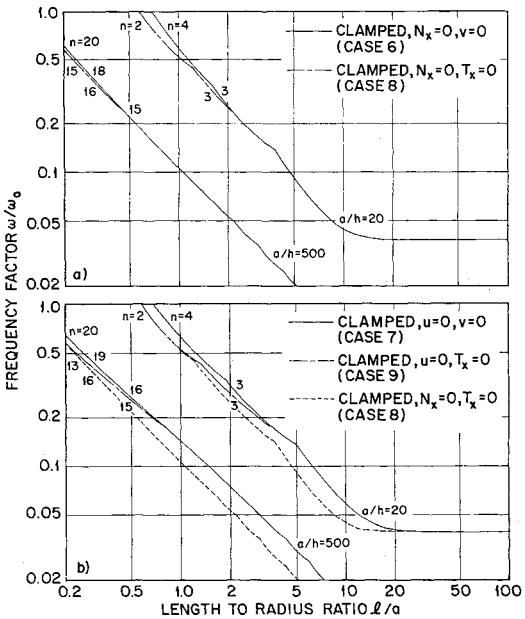

Fig. 7 Frequency envelope, cases 6–9.

out most of the region of interest. This difference may be even greater for certain modes (see Fig. 8). The physical reason for the difference in the influence of $u = 0$ as compared with $\partial w/\partial x = 0$ perhaps can best be understood by examining the modal stress resultants. This will be done in another section. Although the curves on Fig. 4 have been drawn for $m = 1$, the frequencies for modes having one axial node ($m = 2$), for a simply supported shell with axial constraint (case 3), can be determined directly from the intermediate curve (case 2) on Fig. 4. It can be shown that a shell of length $2l/a$, boundary conditions of case 3, and with $m = 2$, has the same modal behavior as a similar shell of length l/a, with $m = 1$ and boundary conditions of case 2. Further study indicates that, no matter what homogeneous boundary conditions are enforced at the ends of the shell, as m increases, the modal characteristics gradually approach those of a simply supported shell without axial constraint (case 1). This trend can be seen (for case 7) in Figs. 8–10.

Arnold and Warburton[5] used the Rayleigh-Ritz procedure to obtain an approximate solution for what they called a shell

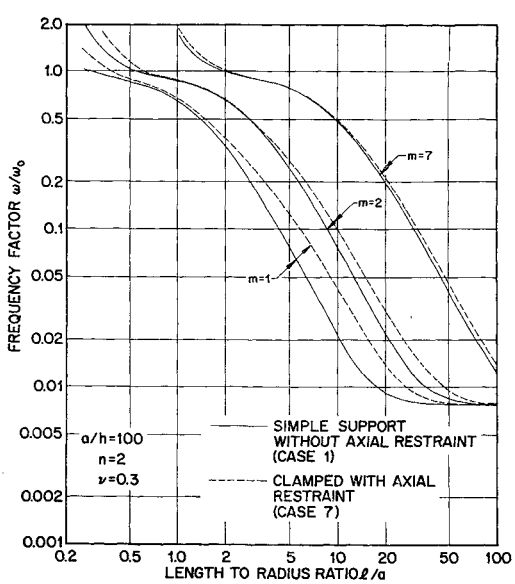

Fig. 8 Frequency distribution for $n = 2$, $m \geq 1$.

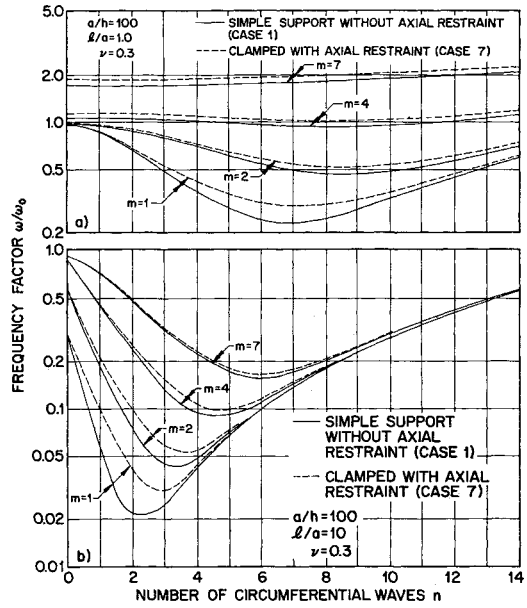

Fig. 9 Frequency distribution for $l/a = 1$ and $l/a = 10$.

with "fixed ends." This is a shell clamped, with axial constraint, at both ends (case 7). Although they took only a one-term approximation to the mode shape, their solution for the frequency agrees very closely with the results of the present analysis (see Fig. 5), theirs being a maximum of 5% higher. For most cases, the results agree within 2%. As is to be expected, however, the modal stress resultants as predicted by their solutions are quite seriously in error. Arnold and Warburton's paper is misleading, however, in so far as it implies that the primary change from the "freely supported" case (studied earlier by them[4]) was the addition of clamping. The effect of elastic moment restraint which they considered must actually be quite small.

In all of the preceding cases, we have assumed that the tangential displacement v is zero. If this requirement is relaxed, with all other parameters remaining the same, the frequency will be lower (see Figs. 6 and 7). The greatest change in the frequency due to relaxing the condition $v = 0$ occurs for $n = 1$. It is important to note at this point that for this boundary condition the minimum frequency may occur for $n = 1$ even for short shells.

Over-All Frequency Pattern

It is not practical to try to compare on a two-dimensional plot the influence of different boundary conditions on the over-all frequency distribution. This was the reason for discussing only the frequency envelope in the preceding figures. In order to understand how these figures relate to the over-all pattern, one case will be studied in more depth. Figure 11 is a three-dimensional plot of the frequency as a function of n and l/a, for a specific shell ($a/h = 100$, $\nu = 0.3$), and for one axial half-wave. Two different sets of boundary conditions are shown: simple support without axial constraint (case 1) and clamped with axial constraint (case 7). Note that the scale for l/a is reversed from the sense used in preceding figures. The minimum curves shown in Fig. 11 are the type of curves plotted in Figs. 3–7.

The difference between the surface for case 1 and the surface for case 7, for $l/a < 1$, is primarily due to the effect of moment restraint. For $l/a > 1$, the difference is due to the effect of axial restraint. The frequencies associated with the various values of n for a fixed l/a are very close in magnitude for short shells, as evidenced by the nearly horizontal grid lines in the n direction. For long shells, the influence of the boundary conditions extends over a much narrower band of circumferential waves.

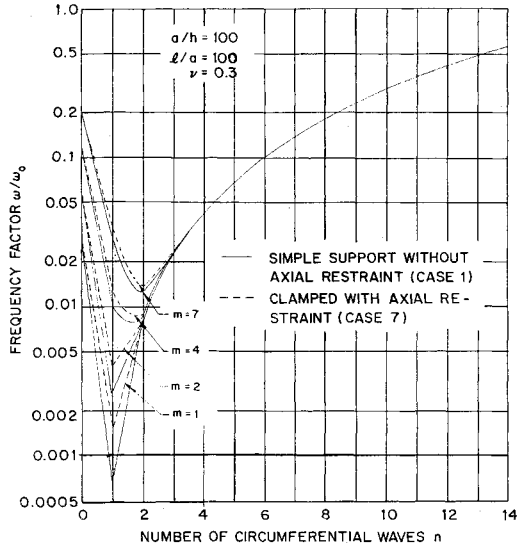

Fig. 10 Frequency distribution for $l/a = 100$.

To further illustrate these points, a cross section of Fig. 11 has been drawn for three different values of l/a (i.e., 1, 10, 100). Figure 9a is the cross section for $l/a = 1$. (Only the $m = 1$ curve appears in Fig. 11.) Note that the value of n for which the minimum frequency occurs depends upon the half-wavelength l/ma. Note also that, for $m = 1$, there are nine values of n which have frequencies less than the minimum value for $m = 2$. For $l/a = 10$ (Fig. 9b), there are three values. Figure 10 shows a change in character of the ordered frequencies. The minimum frequency occurs for $n = 1$, and there are no other values of n which have frequencies less than that for $n = 1$ and $m = 3$. For $n = 2$, there are 10 values of m which have corresponding frequencies that are less than the minimum value for $n = 3$.

The detailed behavior of the higher modes for the entire range of l/a is illustrated in Fig. 8 for $n = 2$. These curves

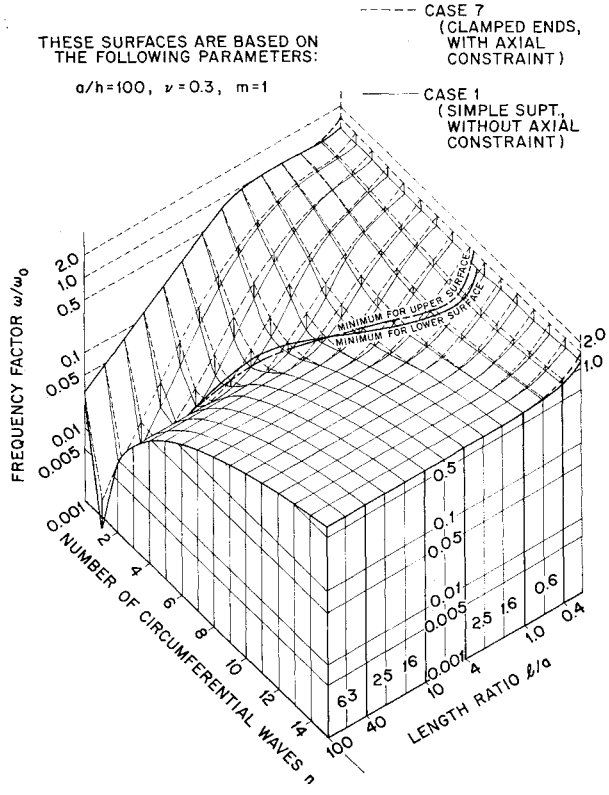

Fig. 11 Over-all frequency pattern for $a/h = 100$.

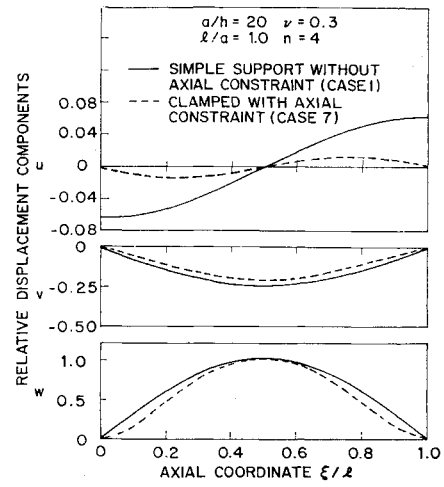

Fig. 12 Mode shape for $a/h = 20$, $l/a = 1$, $n = 4$.

are typical of those obtained for any value of n. The diminishing inuflence of the boundary conditions on higher values of n is clearly seen here. Note also that, for $m = 1$ and $5 < l/a < 15$, the frequency for case 7 is almost 100% higher than for case 1. In this same region, the difference in minimum frequencies is about 50%.

Modal Stress Resultants

A study of selected stress resultants that arise during modal vibration is essential for full understanding of the influence of the various boundary conditions on the modal behavior of thin shells. The results shown in Figs. 12–16 are all for $a/h = 20$. For thinner shells, the moment distribution is not influenced nearly as much by the various boundary conditions and, in fact, is very close to that for a simply supported shell in all cases. The axial force distribution, on the other hand, is essentially independent of a/h.

There is no unique basis for comparing the magnitude of the various stress resultants for different conditions. For our purpose here, the maximum radial deflection has been taken as the normalizing factor. The important items to compare from case to case are not so much the magnitudes of the stress resultants, but rather their distributions.

In Figs. 14 and 15, distributions of both the axial force N_x and the axial moment M_x are compared for two sets of bound-

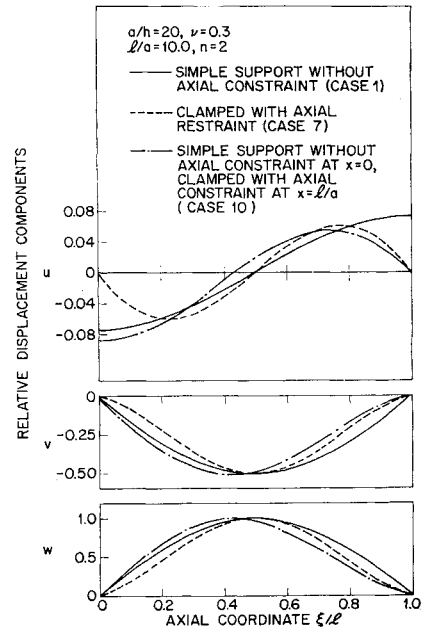

Fig. 13 Mode shape for $a/h = 20$, $l/a = 10$, $n = 2$.

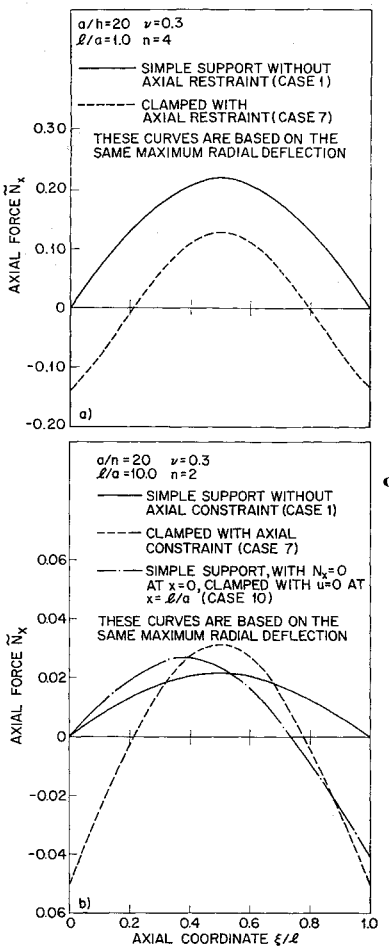

Fig. 14 Distribution of axial force during modal vibration.

ary conditions, cases 1 and 7. From these figures, we can see that the region in which the moment is affected decreases as the shell gets longer. Furthermore, a study of other values of a/h shows that, as the shell becomes thinner, the boundary conditions have less and less influence on the

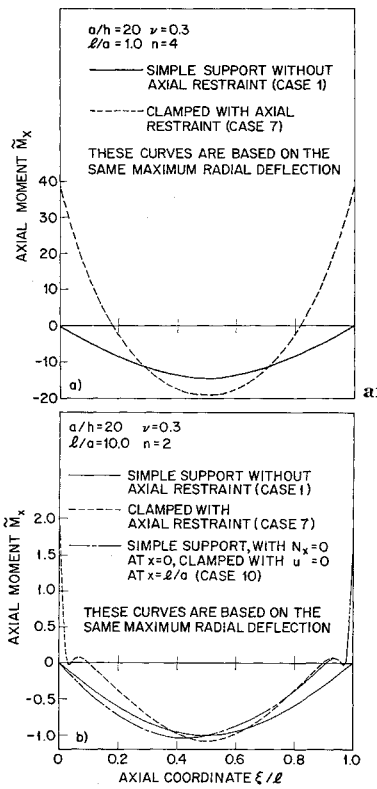

Fig. 15 Distribution of axial moment during modal vibration.

moment distribution. The influence of the condition $\partial w/\partial x = 0$ is generally localized, and this underlies the frequency distribution shown in Fig. 3. The shape of the axial force distribution shown in Fig. 14, on the other hand, could apply to any shell. It is apparent that the boundary condition $u = 0$ always has a strong influence on the axial force distribution, and this contributes to an understanding of the significant increase in the frequency shown in Fig. 4.

Figure 16 rather clearly demonstrates the increasing localization of the effects of the boundary conditions as the number of axial waves increases. This is in accord with the trend already noted in Figs. 8–10.

The difference in behavior of N_x and M_x for the various boundary conditions is similar to the static response of a thin cylindrical shell to various types of edge loading. It has been shown[6] that, for cylindrical shells, certain types of edge loading produce significant stresses only in a very localized boundary zone, whereas other types of loading will propagate far into the interior of the shell.

Conclusions

The present approach provides a powerful tool for examining a wide variety of boundary conditions and their influence on the modal behavior of cylindrical shells. Since no approximations have been introduced beyond those underlying Flügge's equations, the mode shapes, modal accelerations, and modal stress resultants can be computed quite accurately. The results of this study clearly indicate that care must be taken in any approximate analysis to use appropriate boundary conditions.

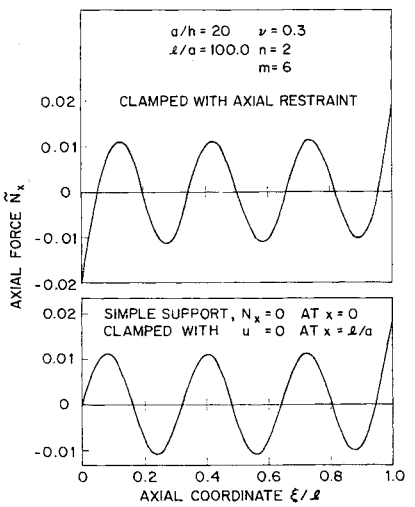

Fig. 16 Distribution of axial force during modal vibration when $m = 6$.

One important question, not studied here, is what constitutes reasonable boundary conditions in actual practice. Although this question is not answered, it is clear that the out of plane stiffness of end rings is far more important, in general, than the resistance of a ring to rotation of its cross section. Furthermore, it is to be noted that a stiff end ring will provide axial restraint for $n \geq 2$, even if the ends of the shell can move axially or rotate as a plane. This indicates that what constitutes axial restraint for $n \geq 2$ may not necessarily be considered axial restraint for $n = 0$ or $n = 1$.

References

[1] Gros, C. G. and Forsberg, K., "Vibrations of thin shells: a partially annotated bibliography," Lockheed Missiles and Space Co., SB 63-43 (1963).

[2] Sobel, L., "Effects of boundary conditions on the stability of cylinders subject to lateral and axial pressures," AIAA J. 2, 1437–1440 (1964).

[3] Flügge, W., *Stresses in Shells* (Springer-Verlag, Berlin, 1960), Chap. 5, pp. 219 and 233.
[4] Arnold, R. N. and Warburton, G. B., "Flexural vibrations of the walls of thin cylindrical shells having freely supported ends," Proc. Roy. Soc. (London) **A197**, 238–256 (1949).
[5] Arnold, R. N. and Warburton, G. B., "The flexural vibrations of thin cylinders," Inst. Mech. Engrs. (London), Proc. Automobile Div. **167**, 62–80 (1953).
[6] Steele, C. R., "Shells with edge loads of rapid variation," Lockheed Missiles and Space Co., TR 6-90-63-84 (1963).

DECEMBER 1964 AIAA JOURNAL VOL. 2, NO. 12

Approximate Laplace Transform Inversions in Viscoelastic Stress Analysis

THOMAS L. COST*
Rohm & Haas Company, Huntsville, Ala

An investigation was made of approximate methods for inverting Laplace transforms that occur in viscoelastic stress analysis when use is made of the elastic-viscoelastic analogy. Alfrey's and ter Haar's methods and Schapery's direct method were examined and shown to be special cases of a general inversion formula due to Widder. Schapery's least squares method and several techniques based on orthogonal function theory were also examined. Viscoelastic solutions to two problems involving deformations and stresses in solid propellant rocket motors under axial and transverse acceleration loads were obtained by use of several of the methods discussed. The problems were typical of the type where the associated elastic solution is known only numerically. The use of the orthogonal polynomial methods is explained in detail, and their limitations discussed. From the investigation described, it was concluded that Schapery's direct method and ter Haar's method generally give good results when applicable. Widder's general inversion formula, which includes Alfrey's method as a special case, is not useable for the type problems of interest here. Although the orthogonal polynomial methods possess characteristics that make them especially suited to the type problems considered, their use appears limited by severe computational difficulties. Schapery's least squares method gives good results to most problems of interest.

Introduction

THE elastic-viscoelastic analogy has been the method most commonly used for obtaining stress distributions and displacements in linear viscoelastic bodies. The analogy has been derived using both a separation of variables technique and an integral transform method. Alfrey[1] was the first to formulate the analogy using the separation of variables technique, whereas Read[2] was first to derive the analogy using Fourier integral transforms. Lee[3] subsequently showed that the analogy could also be derived by use of the Laplace transform. Further developments and extensions have been concisely summarized by Hilton.[4] In the remarks that follow, the elastic-viscoelastic analogy discussed will be the form derived by Lee.[3]

The elastic-viscoelastic analogy can be shown to exist by operating on the field equations, constitutive equations, and boundary conditions of a linear viscoelastic body with the Laplace transform with respect to time. This operation reduces derivatives and integrals with respect to time to algebraic expressions of the transform parameter. The equations that result after this operation are analogous to the field equations, constitutive equations, and boundary conditions that govern the behavior of an elastic body of the same geometry as the viscoelastic body. If the solution to this associated elastic problem can be obtained, the solution to the time dependent viscoelastic problem can be obtained by operating upon the stresses and displacements of the associated elastic problem with an inverse Laplace transform. Thus, the results of the theory of elasticity can be used to obtain solutions to viscoelastic problems.

There are three general classes of problems where an exact form of the elastic-viscoelastic analogy does not apply. The first class consists of problems with moving boundaries where the motion is due to some external source and is entirely different from the usual infinitesimal deformations due to load, temperature, etc. The second class consists of problems where the type of boundary condition at a boundary point changes with time, i.e., a stress boundary condition at a point at one instant of time changes to a displacement boundary condition at another instant of time and vice versa. The third class consists of problems where the compressible material properties are time dependent. If the material properties are time dependent, the differential equations have variable coefficients or the integral equations are not of the convolution type. Thus, the constitutive equations do not reduce to algebraic expressions when operated on with the Laplace (or Fourier) transform.

Although these limitations are serious and exclude from consideration many problems of interest in viscoelastic stress analysis of solid propellant rocket motors, there are still many problems that fall within the realm of application of the analogy which are of interest. Until recently, viscoelastic solutions to problems in which the associated elastic problem was obtained by some numerical technique have been unobtainable by this method because of the difficulty of taking the inverse Laplace transform of functions that are known

Presented as Preprint 64-132 at the AIAA Solid Propellant Rocket Conference, Palo Alto, Calif., January 29–31, 1964; revision received August 4, 1964. This work was conducted for the Army Ordnance Corps under contract number DA-01-021-ORD-11878(Z).

* Intermediate Scientist, Applied Mechanics Group, Engineering Research Section, Redstone Arsenal Research Division.